JACC Vol. 6, No. 1
July 1985:55–63

METHODS

Evaluation of Aortic Stenosis by Spectral Analysis of the Murmur

GARY R. JOHNSON, MD,*†‡ GORDON S. MYERS, MD, FACC,*† ROBERT S. LEES, MD, FACC*†‡

Boston and Cambridge, Massachusetts

A relation between the peak transaortic pressure gradient and the frequency content of the murmur (r = 0.79) was demonstrated in a prospective "test" set of 50 patients with the clinical diagnosis of aortic stenosis. After heart sounds were recorded and digitized, three segments of the systolic murmur were isolated and analyzed by fast Fourier transform technique. An average frequency spectrum was quantitated by a previously described empiric spectral estimator. Clinical data and spectral ratio were correlated with the transaortic pressure gradient and aortic valve area was calculated from cardiac catheterization data. The best prediction of the transaortic pressure gradient was obtained when a 170 ms murmur segment was analyzed and when the predictive algorithm also included the aortic dimension (r = 0.87). The aortic valve area was poorly predicted (r = −0.48) unless estimates of blood flow and valvular calcification were included in the algorithm (r = 0.84). Further refinement of this technique may provide a noninvasive and clinically useful method for the estimation of aortic valve stenosis.

(J Am Coll Cardiol 1985;6:55–63)

Assessment of the severity of valvular aortic stenosis remains a common problem. Because clinical criteria have not been sufficiently reliable (1–5), a number of noninvasive techniques have been used to estimate the severity of aortic stenosis. Phonocardiographic (6–10), electrocardiographic (11) and echocardiographic (12–15) algorithms have been devised but have not provided accurate predictions of aortic valve pressure gradients. More recently, quantitative Doppler techniques (16–19) have achieved significant success in predicting peak aortic valve gradients. Continuous wave Doppler methods are capable of measuring the high velocity transvalvular blood flow present in aortic stenosis, but they lack range resolution and usually fail to provide two-dimensional orientation for the examiner. Pulsed Doppler techniques permit localization of flow disturbances but are limited in their ability to measure high flow velocities accurately. Furthermore, the use of equipment combining continuous wave and pulsed Doppler methods involves expensive and complex instruments, sophisticated and experienced operators and cooperative patients with adequate "acoustic windows."

In a previous study (20) of 23 patients with a clinical diagnosis of aortic stenosis, we introduced a new approach to the noninvasive estimation of the peak aortic pressure gradient. The murmurs produced by the stenosis were recorded at the skin surface and analyzed. The mean frequency spectrum of the aortic systolic murmur was derived, and an empiric spectral estimator was calculated as the ratio of the area under the curve between 75 and 150 Hz to the area between 25 and 75 Hz. The spectral ratio correlated with the peak to peak gradient measured across the aortic valve at cardiac catheterization (r = 0.90).

Our study was designed to evaluate the spectral ratio prospectively in a larger group of patients.

Methods

Patient group. The 50 consecutive patients studied were 67 ± 10 years of age (mean ± SD, range 41 to 84) and had been referred for diagnosis of aortic valve disease at the Massachusetts General Hospital and the New England Deaconess Hospital. Twenty-eight patients were male, aged 65 ± 10 years and 22 patients were female, aged 70 ± 9 years. Informed consent was obtained from each patient studied according to the study protocols approved by the Human Studies Section, Committee on Research at the Massachusetts General Hospital and the Committee for Clinical Investigation at the New England Deaconess Hospital.

The following patient data were collated: age; sex; blood

From the Departments of Medicine, *New England Deaconess Hospital, Harvard University, Cambridge, Massachusetts and †Massachusetts General Hospital, Boston, Massachusetts and ‡Department of Nutrition and Food Science, Massachusetts Institute of Technology, Cambridge, Massachusetts. This study was supported in part by grants from the Whitaker Health Sciences Fund of Massachusetts Institute of Technology, Cambridge, Massachusetts and the Ambrose Monell Foundation, New York, New York and by private donations. Manuscript received September 24, 1984; revised manuscript received January 21, 1985, accepted February 1, 1985.

Address for reprints: Gary R. Johnson, MD, 110 Francis Street, Suite 7H, Boston, Massachusetts 02215.

0735-1097/85/$3.30

pressure; heart rate; presence of syncope, angina pectoris or congestive heart failure; results of the electrocardiogram, chest radiograph and cardiac fluoroscopy and complete blood count. The electrocardiogram was examined for arrhythmias and for evidence of left ventricular hypertrophy. The chest radiograph was evaluated for the presence of left ventricular enlargement and vascular redistribution.

Sound acquisition. A standard phonocardiographic microphone with a 1.5 cm^2 pedestal (Hewlett-Packard HP 21050A) was used for skin surface heart sound recordings. The frequency response of this microphone is flat from 1 to 700 Hz and decreases by 3 dB/octave from 700 to 1,500 Hz (21). In a previous study (22), we devised a special holder to control the force applied by the microphone to the chest wall. In addition, we found over a range of 5 to 750 g that the signal amplitude for any given location on the thorax increased with increased force to a maximum between 300 and 600 g (unpublished data on the quantitative effects of transducer application to the human chest wall). Therefore, we chose a standard microphone force of 500 g for our study.

The patients were evaluated within a week of the time of cardiac catheterization. Sound recordings were obtained in a quiet room with the patient supine and during held expiration. No patient was excluded from this study because of inability to obtain a satisfactory sound signal. The microphone in its special holder was positioned initially on the chest wall in the second right intercostal space and subsequently in the second left intercostal space. A simultaneous electrocardiogram was recorded for timing of the cardiac sounds.

The signals from the microphone were amplified with a preamplifier (Princeton Applied Research model 113); its band pass filter was set at 30 and 1,000 Hz. This filter rolls off at 6 dB/octave less than 30 and greater than 1,000 Hz. The recordings were stored on a TEAC 2300 SX reel to reel tape recorder, which has a flat frequency response between 40 and 1,500 Hz.

The recorded heart sounds were further filtered by a high rejection (80 dB/octave) 30 to 1,500 Hz band pass Rockland 751A filter before analog to digital conversion. The 30 Hz setting was used to eliminate low frequency noise and the 1,500 Hz setting to prevent aliasing during sampling. The magnitude of the sound signal was adjusted to use the full analog to digital conversion range and then sampled at 3,000 Hz. A Nova-4 computer (Data General, Inc.) was used to sample, store and analyze the signal.

Murmur selection. After the sound signal and simultaneous electrocardiogram were digitized, the computer program selected and displayed a cardiac cycle including the first heart sound, systolic ejection murmur, second heart sound and diastolic murmur, if present, along with the simultaneous electrocardiogram. The desired portion of the cardiac cycle was chosen by the operator and displayed on the computer screen; the computer program then selected the corresponding time window from 6 to 10 stored cardiac cycles, using the electrocardiogram as a time reference. In patients with atrial fibrillation or other significant arrhythmia, 10 to 15 cardiac cycles were examined by the operator and the desired portion of each cycle was selected manually.

After the preliminary selection, each segment was refined by the operator according to the following criteria: the duration of the first heart sound was judged to be 90 to 110 ms and sometimes was followed by vibrations of increased amplitude thought to represent an ejection sound. However, the beginning of the systolic ejection murmur was defined as the point closest to zero amplitude after the first heart sound, and the end of the systolic ejection murmur as the lowest amplitude point immediately preceding the second heart sound.

The computer program allowed the selection of three discrete time windows for analysis. Because the fast Fourier transform spectral analysis required a preset number of sample points, the time window durations were 86 ms, representing 256 sample points; 170 ms, representing 512 sample points and 341 ms, representing 1,024 sample points. The typical relation of these sample lengths to the cardiac cycle is shown in Figure 1. As illustrated, the 86 ms window was centered on the peak of the murmur, whereas the 170 ms window included most or all of the systolic murmur in all patients. The latter window did not include the first or the second heart sound. The 341 ms window, which was used for comparison with the previous study (20), encompassed all of systole and the second heart sound in the majority of cases.

Frequency spectra. Six to 10 cardiac cycles for each patient at each of the two recording sites were then analyzed

Figure 1. Typical phonocardiogram (PCG) of the murmur of aortic stenosis with simultaneous electrocardiogram (ECG). The three time windows used for the spectral analysis (86 ms, 170 ms and 341 ms) are indicated, as are the first heart sound (S_1), second heart sound (S_2) and systolic ejection murmur (SEM).

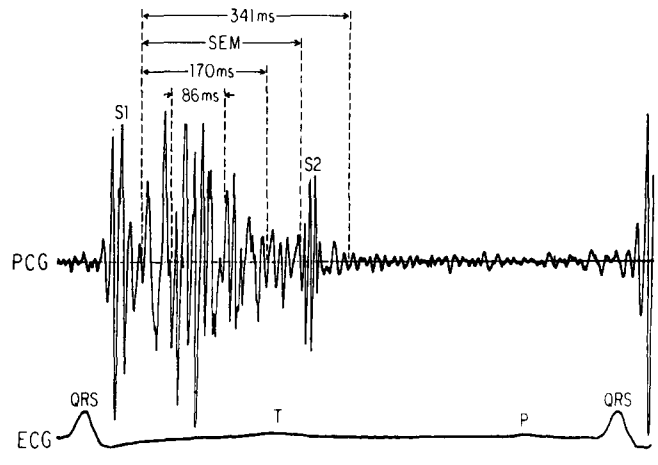

by fast Fourier transform technique and the frequency spectra were averaged. A mean spectrum for each patient at each sample length and recording site was calculated.

The spectral estimator (spectral ratio) (20) was then derived from each spectrum. This empiric algorithm was designed to estimate the relative frequency content of the systolic murmur and was defined by the following equation:

$$PA/CA = \frac{\int_{75}^{150} A(f)df}{\int_{25}^{75} A(f)df}, \quad [1]$$

where PA = predictive area; CA = control area; A(f) is the signal amplitude in millivolts at each frequency (f) in Hz and df is the derivative with respect to f. Amplitudes considered to be noise (≥ 40 dB below the predominant frequency) were not included in the calculation of the spectral ratio. All results are rounded to the nearest tenth. Two examples of heart sounds, corresponding electrocardiograms, derived mean frequency spectra, and spectral ratios are shown in Figure 2.

A study of the reproducibility of the spectral ratio was conducted by two investigators who independently chose 6 to 10 cardiac cycles from the recorded data to analyze in the first 30 of the 50 patients studied. Time window segments of 170 ms duration were selected by the criteria just described, and spectral ratio values were derived from the resulting spectra.

Figure 2. Representative phonocardiograms (PCG), electrocardiograms (ECG) and the derived mean frequency spectra and spectral ratios are displayed for a patient with a low gradient (G) (**left**) and one with a high gradient (**right**). The **vertical dash lines** on the frequency spectra represent the limits (25, 75 and 150 Hz) used to calculate the spectral ratio. PA/CA = predictive area/control area = spectral ratio.

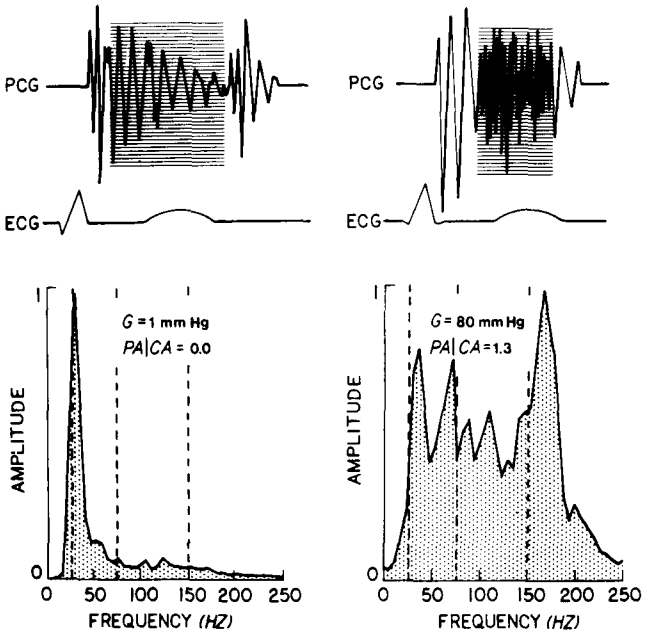

Invasive data acquisition. All patients underwent cardiac catheterization. The hemodynamic data obtained included left ventricular systolic and end-diastolic pressures, aortic systolic and diastolic pressures and peak to peak and mean transvalvular gradients. The aortic valve area was calculated by the Gorlin formula (23). In two patients with a significant gradient and 2+ or greater aortic regurgitation, valve areas were not calculated. Other data obtained at catheterization included heart rate, ejection fraction by planimetry of the left ventriculogram, cardiac output/index by the Fick method, degree of ventricular dyskinesia, stroke volume, degree of valvular calcification on a scale of 0 to 4, the aortic root dimension 2.5 cm above the aortic anulus, an estimate of aortic regurgitation by injection of contrast medium above the aortic valve on a scale of 0 to 4 and coronary angiography. All data are collated in Table 1.

Statistical analysis. All data were stored on a Vax 11-780 computer. Statistical analyses were performed with the University of California, Los Angeles Biomedical Data Package (24) and the following were determined: mean, standard deviation and coefficient of variation. Groups were compared statistically by unpaired *t* tests with and without the assumption of equality of variance (25). Multivariate analysis used the Furnival-Wilson algorithm. The "best" multivariate regression estimates were selected by Mallow's criteria (25).

Results

Clinical features. Angina pectoris, congestive heart failure or syncope was found in all 50 patients studied (Table 2). Syncope was more common in women than in men (32 versus 14%) ($p < 0.01$). No significant difference in the incidence of angina pectoris or congestive heart failure was found between the sexes.

For this group of patients, the following values (mean ± SD) were found: aortic systolic blood pressure 142 ± 31 mm Hg, diastolic pressure 65 ± 11 mm Hg, pulse pressure 76 ± 26 mm Hg and hematocrit 38 ± 4%. Twenty-six of the 50 patients had systolic hypertension (≥ 140 mm Hg); none had diastolic hypertension (≥ 95 mm Hg). Electrocardiographic evidence of left ventricular hypertrophy was found in 56% of the patients, and left ventricular enlargement by X-ray study was noted in 58%. The degree of valvular calcification, as estimated by image intensification fluoroscopy, was 2.8 ± 1 (scale 0 to 4).

Angina, congestive heart failure, syncope and standard laboratory results were compared with each other and with each of the invasive estimates of aortic stenosis severity (mean and peak transvalvular pressure gradients and aortic valve areas). All of these variables were poorly correlated ($r \leq 0.4$).

Table 1. Demographic, Hemodynamic and Acoustic Data From 50 Patients

Case	Age (yr) & Sex	Sync	AP	CHF	BP (mm Hg)	Rhy	ECG LVH	CXR LVE	LVD	EF (%)	Ca^{+2}	AD (cm)	AR	LV SP/EDP	PG/MG (mm Hg)	CO (liters/min)	AVA (cm^2)	PA/CA
1	62M	+	+	+	135/75	S	0	0	+	62	2	2.6	0	160/8	40/30	6.4	1.3	0.8
2	74M	+	+	+	110/60	S	+	0	0	65	2	3.5	0	200/16	90/80	5.5	1.0	2.8
3	75F	0	0	+	105/50	S	+	+	+	25	4	3.5	0	190/22	85/65	3.5	0.3	2.5
4	65M	0	+	+	150/60	S	0	+	0	63	4	2.9	1	225/15	75/60	7.5	1.0	2.2
5	69M	0	0	+	120/65	S	0	0	+	73	4	3.2	0	175/8	55/40	5.9	0.9	1.7
6	68F	0	0	+	140/60	S	+	+	0	82	3	4.3	0	260/8	130/120	4.9	0.4	2.0
7	83M	0	0	+	150/64	AF	+	+	0	31	4	3.4	0	95/6	55/35	2.5	0.3	1.2
8	74F	+	+	+	140/50	S	+	+	0	55	4	3.4	1	225/7	85/70	4.6	0.6	1.2
9	74F	0	0	+	164/73	S	0	+	0	50	4	2.9	0	220/13	58/40	6.0	0.8	1.0
10	60M	0	0	+	125/65	S	+	0	+	55	3	2.9	0	210/3	90/40	4.3	0.5	2.4
11	51M	0	0	0	130/60	S	+	+	0	60	2	3.1	2	200/10	70/45	9.2	–	1.7
12	72F	0	+	+	90/55	S	+	+	0	20	4	2.8	0	190/9	100/68	4.6	0.3	2.0
13	62M	0	0	+	125/70	S	+	0	0	30	2	2.5	0	215/11	140/90	5.9	0.4	3.2
14	56M	0	+	+	130/60	S	+	+	0	60	4	5.2	0	235/23	90/75	6.4	0.6	0.6
15	53F	+	+	+	115/50	S	0	+	0	50	4	3.2	0	195/25	80/75	4.4	0.4	2.4
16	73F	0	+	0	178/63	S	+	0	0	78	2	3.7	0	192/8	14/10	3.1	1.3	0.5
17	77F	+	+	+	160/50	S	+	+	+	62	2	2.7	0	200/10	40/30	3.7	0.7	0.8
18	46F	+	0	0	126/46	S	0	+	+	71	0	2.2	2	126/5	1/1	2.9	–	0.0
19	75M	0	0	+	210/72	S	0	0	+	31	4	2.5	0	230/31	20/12	5.1	0.6	0.3
20	57M	0	+	0	170/90	S	+	+	0	69	2	2.0	0	190/16	20/15	3.1	0.8	0.8
21	77M	0	+	+	94/50	S	0	+	0	53	4	3.0	0	107/14	14/10	3.2	1.0	0.9
22	62M	0	+	0	165/70	S	0	0	+	85	0	2.6	0	165/12	1/1	4.5	–	0.0
23	72M	0	+	0	168/80	S	+	+	+	58	2	2.9	0	165/15	65/55	4.2	0.6	1.3
24	53M	0	0	+	150/80	S	+	0	0	60	4	2.4	0	220/10	70/56	5.5	0.9	1.1
25	71F	0	0	+	120/60	S	0	+	0	81	3	4.0	0	195/2	50/50	2.9	0.4	0.9
26	61F	0	0	+	106/70	S	+	+	0	81	4	4.3	0	200/10	94/75	4.8	0.3	1.6
27	78M	0	0	+	110/50	S	+	0	0	66	3	3.1	0	140/14	50/30	5.1	1.0	1.7
28	61M	0	+	+	150/75	S	0	+	0	50	3	2.9	0	230/4	80/50	6.6	0.7	1.7
29	57F	0	0	+	132/60	AF	0	+	0	60	1	2.1	1	132/18	2/2	4.4	–	0.4
30	51M	0	+	+	85/60	S	+	+	+	55	2	2.8	0	120/12	35/20	4.3	0.9	1.6
31	65M	0	+	0	160/63	S	+	0	+	60	3	3.3	0	195/11	35/25	5.8	0.8	0.4
32	65F	+	+	+	165/65	S	+	0	0	71	3	2.9	3	200/17	35/31	4.2	–	0.8
33	84F	0	0	0	100/80	S	+	+	+	48	4	3.3	0	200/10	100/10	3.7	0.2	1.8
34	70F	0	0	+	140/70	AF	0	+	+	41	4	2.3	0	140/10	0/0	2.3	–	0.6
35	56M	0	+	0	110/65	S	+	+	+	43	3	3.4	0	170/16	100/60	4.1	0.5	1.3
36	69F	+	+	+	170/80	AF	+	+	+	52	4	4.3	0	290/25	120/80	4.3	0.3	1.3
37	68M	0	0	0	180/90	S	0	0	0	52	3	4.3	0	270/25	90/65	3.6	0.4	0.6
38	71M	0	+	0	160/60	S	+	+	0	69	3	3.3	0	210/26	48/36	4.6	0.7	0.6
39	74F	0	+	0	185/85	S	0	0	+	55	4	2.2	0	215/30	25/18	4.1	0.7	0.9
40	41M	0	+	0	150/74	S	+	+	+	60	0	2.0	3	150/10	0/0	8.2	–	0.04
41	72M	+	0	0	210/80	S	0	+	0	55	0	2.0	0	220/8	10/6	5.6	1.5	0.8
42	72M	0	0	0	150/65	S	0	0	0	68	1	2.3	0	160/5	10/8	4.4	1.2	0.0

Table 1. *(continued)*

Case	Age (yr) & Sex	Sync	AP	CHF	BP (mm Hg)	Rhy	ECG LVH	CXR LVE	LVD	EF (%)	Ca^{+2}	AD (cm)	AR	LV SP/EDP	PG/MG (mm Hg)	CO (liters/min)	AVA (cm^2)	PA/CA
43	73M	0	0	+	135/74	S	+	+	+	–	4	5.0	0	210/27	75/53	4.1	0.4	1.5
44	78F	0	+	+	200/80	S	+	+	+	58	3	2.7	0	240/8	47/36	5.8	0.8	0.5
45	70F	0	0	0	200/80	S	+	0	0	60	4	2.6	0	245/22	44/22	3.2	0.5	0.4
46	72M	+	0	0	115/50	S	0	0	+	50	4	2.5	0	215/10	100/89	4.2	0.4	2.2
47	77F	0	0	0	150/65	AF	0	0	0	55	3	2.5	0	173/10	23/16	–	–	0.6
48	58M	0	0	0	120/80	S	0	0	+	35	3	2.4	0	152/8	32/20	4.0	0.7	0.7
49	74F	+	0	0	235/90	S	0	0	0	65	2	2.6	0	270/16	35/31	4.7	0.7	1.2
50	70F	0	+	0	120/70	S	0	0	+	77	4	1.9	0	200/6	80/62	2.6	0.5	1.3

AD = aortic dimension; AF = atrial fibrillation; AP = angina pectoris; AR = aortic regurgitation; AVA = aortic valve area calculated by the Gorlin formula; BP = blood pressure; Ca^{2+} = valvular calcium; *CHF = congestive heart failure; CO = cardiac output; CXR = chest radiograph; ECG = electrocardiogram;* EF = ejection fraction; LV = left ventricle; LVD = left ventricular dyskinesia; LVE = left ventricular enlargement; LVH = left ventricular hypertrophy; PA/CA = spectral predictor; PG/MG = peak gradient/mean gradient; Rhy = rhythm; S = sinus; SP/EDP = systolic pressure/end-diastolic pressure; Sync = syncope.

Table 2. Summary of Major Signs and Symptoms of 50 Patients

	Angina Pectoris (AP)	Congestive Heart Failure (CHF)	Syncope (Sync)
Single clinical abnormality	15	15	4
AP +	–	7	1
CHF +	7	–	0
Sync +	1	0	–
AP + CHF + Sync	8	8	8
Total patients with each sign or symptom	31	30	13

Invasive data. The hemodynamic data are summarized in Table 3. The cardiac output/index (2.3/1.2 to 9.2/4.8 liters/min), as well as the pressure gradients (0 to 140 mm Hg), were distributed over the usual range of clinically observed values (Fig. 3). The invasive indexes of severity of stenosis, aortic valve area and mean and peak gradients correlated poorly ($r < 0.5$) with the other hemodynamic data.

Forty-three patients were studied by coronary angiography and left ventriculography. Twenty-two patients had significant coronary artery disease (≥ 50% diameter stenosis) and 21 patients had an abnormal ventriculogram. No association was found between the presence of significant coronary artery disease or myocardial dysfunction and the severity of aortic stenosis. Combined aortic regurgitation and stenosis was present in five patients; two of these had grade 2 to 3 regurgitation and three had grade 1. Valve areas were not calculated in the two patients with grade 2 to 3 aortic regurgitation, and in one patient because cardiac output was unavailable. In five patients without a detectable gradient, the valve area was approximated by the internal diameter of the aortic root measured from the aortogram.

Table 3. Hemodynamic Data From Cardiac Catheterization

	Mean ± SD	Range
Cardiac output (liters/min)	4.7 ± 1.4	2.3 to 9.2
Cardiac index (liters/min per m^2)	2.5 ± 0.7	1.2 to 4.8
Heart rate (beats/min)	73 ± 11	55 to 96
Stroke volume (ml/min)	66 ± 21	25 to 119
Aortic dimension (cm)	3 ± 0.8	1.9 to 5.2
LVSP (mm Hg)	195 ± 42	95 to 290
LVEDP (mm Hg)	13 ± 7	2 to 31
Peak transaortic pressure gradient (mm Hg)	57 ± 37	0 to 140
Mean transaortic pressure gradient (mm Hg)	42 ± 29	0 to 120
Aortic valve area (cm^2)	0.9 ± 0.6	0.24 to 2.5
Ejection fraction (%)	58 ± 15	20 to 85

LVEDP = left ventricular end-diastolic pressure; LVSP = left ventricular systolic pressure.

JACC Vol. 6, No. 1
July 1985:55-63

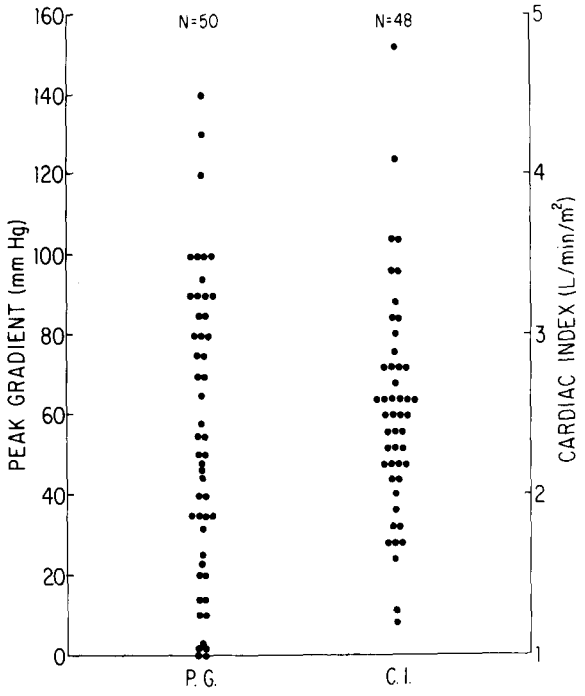

Figure 3. The range and dispersion of the peak transvalvular aortic predicted gradients (P.G.) and the cardiac indexes (C.I.) are displayed.

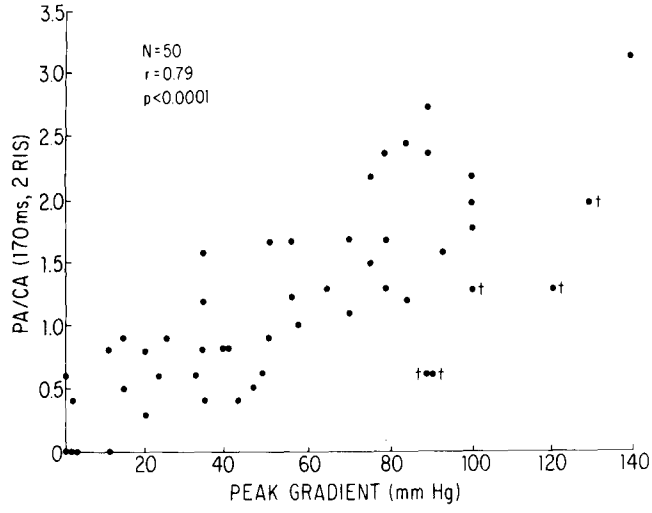

Figure 4. The spectral estimator (the PA/CA ratio [predictive area/control area]) is plotted against the peak transvalvular aortic gradient measured at cardiac catheterization. The patients with an unexpectedly low spectral ratio and significant poststenotic dilation are noted (†).

Sound analysis. Three different sample sizes were analyzed for signals recorded at the second right intercostal space. The correlations of the spectral ratios derived from the three time windows described previously and the invasive severity estimates are shown in Table 4. The best correlation was found when the spectral ratio was calculated from the spectral data derived from the 170 ms time window and is plotted against the peak to peak pressure gradient in Figure 4 ($r = 0.79$, $p < 0.0001$). The points corresponding to patients with poststenotic dimensions of 4.5 to 5.0 cm are identified in Figure 4.

When the spectral ratio, derived from signals recorded from the second left intercostal space with the 170 ms time window, was compared with the invasive variables listed in Table 4, the correlations were not as high as those obtained from the recordings made in the second right intercostal space. Therefore, the predictive accuracy of the spectral estimator in this study depended on the recording location.

Table 4. Correlation of Spectral Ratio Obtained From Murmur Segments of the Indicated Duration With Hemodynamic Data

Sample Duration and Recording Location	Peak Gradient (mm Hg)	Mean Gradient (mm Hg)	Valve Area (cm^2)	Log Valve Area (cm^2)
341 ms (2RIS)	0.72	0.65	−0.39	−0.45
170 ms (2RIS)	0.79	0.76	−0.48	−0.54
170 ms (2LIS)	0.68	0.64	−0.37	−0.43
86 ms (2RIS)	0.47	0.42	−0.22	−0.34

2LIS = second left intercostal space; 2RIS = second right intercostal space.

We tested for the variables that affected the correlation between the spectral ratio and the invasive variables of severity. The "best" equation by Mallow's criteria (recording at second right intercostal space, time window of 170 ms) was as follows:

$$G = 32(\text{spectral ratio}) + 21(\text{aortic dimension}) - 44, \quad [2]$$

where G = peak gradient (mm Hg) and the aortic dimension is in centimeters. The transaortic valve gradients predicted by this equation correlated well with the peak gradients measured at cardiac catheterization ($r = 0.87$, $p < 0.0001$) (Fig. 5). No significant difference was found between the heart rate at the time of sound recording (73 ± 12 beats/min) and the heart rate at the time of cardiac catheterization (74 ± 10 beats/min). The reproducibility study of the spectral ratio yielded a coefficient of variation of 9%. The spectral ratio (second right intercostal space, 170 ms) correlated poorly with the valve area ($r = -0.48$) and with the logarithm of the valve area ($r = -0.54$) (Table 4).

Aortic valve area. Because the spectral ratio is highly correlated with the mean gradient ($r = 0.76$), we replaced the mean gradient in the Gorlin formula for the aortic valve area (AVA) with the spectral ratio and recalculated the valve areas. Eight patients, in whom either the transvalvular aortic pressure gradient was negligible, significant aortic regurgitation was present or the cardiac output was not available, were not included in this predictive analysis.

$$AVA = 0.13 + \frac{0.003 \times (\text{flow/sec systole})}{PA/CA} \quad [3]$$

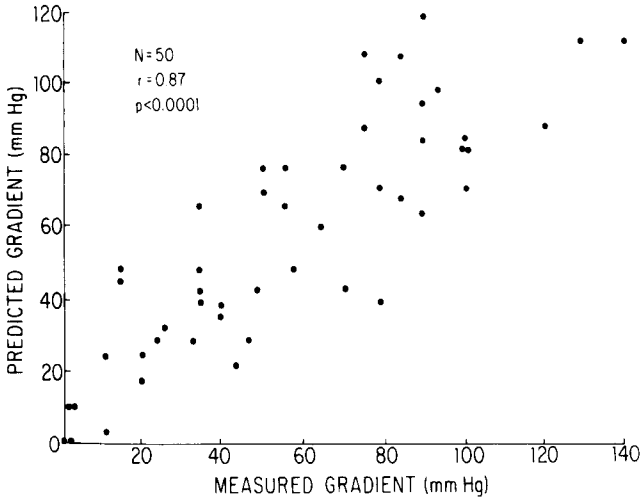

Figure 5. The peak transaortic valve gradient, measured at cardiac catheterization, is plotted against the gradient predicted from the spectral ratio and the aortic dimension (equation 2).

The valve area predicted by equation 3 correlated with the valve area derived from cardiac catheterization with a correlation coefficient of 0.80. In our study valvular calcification was significantly related to valve area ($r = -0.64$, $p < 0.0001$). If the degree of aortic valve calcification (AVC) was included in the predictive algorithm (equation 4), the correlation improved ($r = 0.84$, $p < 0.0001$; Fig. 6):

$$AVA = 0.58 + \frac{0.016 \times (\text{flow/sec systole})}{PA/CA} - 0.1 \times AVC. \quad [4]$$

Figure 6. The valve area calculated from hemodynamic data is plotted against that predicted by equation 4 (inclusion of valvular calcification). Not included in this figure are patients with significant aortic regurgitation and those with valve areas which could not be calculated by the Gorlin formula (see text for details). + = patients with an unexpectedly low spectral ratio and significant poststenotic dilation.

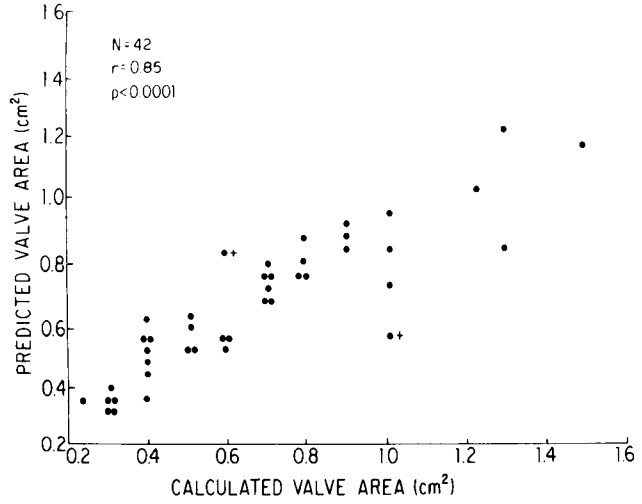

We classified the severity of aortic stenosis as minimal (>1.2 cm²), moderate (>0.7 to ≤1.2 cm²) or severe (<0.7 cm²). Using this classification, the spectral ratio alone predicts the valve area as minimal, moderate or severe in only 29 of the 47 patients (Table 5). When an estimate of flow, such as the invasive estimate of the stroke volume and the degree of valvular calcification, is included in the algorithm, the correct classification was made in 35 of the 47 patients.

Discussion

Advantages of spectral analysis method. We have shown a significant association between the peak transvalvular pressure gradient, ranging from 0 to 140 mm Hg, and the frequency spectrum of the systolic murmur in aortic stenosis. The predictive algorithm we devised was improved by including an aortic root dimension. Among other noninvasive methods, Doppler techniques are currently the most promising, but practical difficulties include obtaining an adequate acoustic window, measuring the angle of insonation accurately and operating within the limited dynamic range of available instrumentation. In addition, Doppler echocardiography is time-consuming, demands considerable operator sophistication and experience and is technically impossible in 5 to 10% of patients (16–18). Spectral analysis of heart sounds, by contrast, requires less skill and time for data acquisition and analysis and was possible in 100% of patients in our study. Our spectral analysis method has been semiautomated and requires about 5 minutes to perform. An entire examination including data acquisition and spectral analysis lasts approximately 15 to 20 minutes, even in patients with atrial fibrillation.

Correlation with clinical features. The average age of our patients (67 years) was somewhat greater than that of patients in many other studies, but the frequency of symptoms in our patients was similar to that reported elsewhere (8,25–30). A significant correlation between the severity of stenosis and the presence of symptoms was not found. However, this statistical dissociation probably reflects a bias in selecting symptomatic patients for catheterization: all patients in our study had angina, congestive heart failure or syncope, alone or in combination.

Pulse pressures from these patients correlated minimally ($r = -0.4$) with the severity of stenosis and were insignificantly affected by the other variables examined. Eliminating the patients with aortic regurgitation from analysis did not significantly affect these correlations. Our results confirm that, although a narrow pulse pressure may be associated with aortic stenosis, normal or wide pulse pressures do not exclude severe aortic obstructive disease. For example, patients in our study with peak gradients of 100 to 140 mm Hg had pulse pressures of 40 to 90 mm Hg. Therefore, in elderly patients the pulse pressure may depend more on the compliance of the arterial tree than on the aortic valve

Table 5. Sensitivity and Specificity of Univariate and Multivariate Prediction of Valve Area

Calculated AVA	True Positive Results	False Positive Results	True Negative Results	False Negative Results	Sensitivity (%)	Specificity (%)
Prediction of Aortic Valve Area (AVA) by Spectral Ratio Alone (n = 49)						
($\leq$0.7 cm^2)	15	6	21	7	68	78
(>0.7 to $\leq$1.2 cm^2)	5	3	29	12	29	91
(>1.2 cm^2)	9	11	29	0	100	72
Overall*					60	80
Prediction of AVA by Systolic Flow/Spectral Ratio and Aortic Valve Calcification (AVC) (n = 44)						
($\leq$0.7 cm^2)	20	1	16	7	74	94
(>0.7 to $\leq$1.2 cm^2)	13	8	22	1	93	73
(>1.2 cm^2)	2	0	41	1	67	100
Overall*					76	90

*The sensitivity and specificity are indicated for the combined groups.

gradient, particularly in the absence of congestive heart failure.

Methodologic considerations. In this and the previous study (20), the frequency content of the murmur of aortic stenosis was more closely related to the peak to peak pressure gradient than to the other invasive variables. In this "test set" of 50 patients, the correlation of the peak transaortic pressure gradient with the spectral ratio, obtained from a phonocardiographic segment of 341 ms duration, was not as high (r = 0.72) as the previously reported correlation (r = 0.90) for the "training set" of 23 patients (20). However, two other time windows in the cardiac cycle were investigated. An 86 ms time window centered at the peak of the systolic murmur yielded data that gave a poor correlation (r = 0.47). Some murmurs contained high amplitude ejection sounds that affected the location of the murmur peaks. Therefore, the 86 ms time window centered on the murmur peak may have included a higher percent of nonspecific data. A 170 ms time window that excluded both the first and second heart sounds proved useful for prediction of peak aortic pressure gradients (r = 0.79); when the aortic dimension was included in the algorithm, prediction improved significantly (r = 0.87). Our results, and data from engineering models to aortic stenosis (31), suggest that an increase in the aortic dimension may decrease the intensity and frequency of the murmur produced by aortic stenosis.

Calculated estimates of the severity of aortic stenosis (23) on the basis of invasive data are affected by several variables. The most important of these are the contractile state of the myocardium, blood velocity and acceleration, arterial impedance and estimate of blood flow across the aortic valve. The spectral ratio alone correctly predicted the hemodynamically estimated valve area (Table 5) in only 29 of 49 patients. When an estimate of flow was included in the algorithm, the prediction of stenosis improved; inclusion of an estimate of valvular calcification further increased the correlation coefficient.

Data most predictive of the severity of aortic stenosis were derived from the systolic murmur recorded in the second right intercostal space; however, the best location for recording heart sounds probably varies from patient to patient.

Limitations. Several aspects of the spectral ratio as defined in this study limit its general applicability: 1) the ratio is extremely variable when the highest amplitude frequencies are near the dividing frequency (75 Hz); 2) the algorithm for the calculation of the spectral ratio does not include a noise rejection function; 3) the frequency components of the murmur that were found to be predictive are not selectively weighted; and 4) interobserver variability (9%) is suboptimal.

We propose to refine further our technique of spectral analysis by individualizing the location of the microphone on the chest wall to obtain the best signal to noise ratio in each patient, converting the unfiltered signal directly from analog to digital form and, eventually, developing improved spectral estimators of the extent of stenosis. The addition of digital signal filtration may facilitate identification of the first heart sound, an ejection click when present, a systolic ejection murmur and the second heart sound.

Clinical implications. Although gross differences in the murmur of mild and severe stenosis may be appreciated by auscultation, the ear is relatively insensitive (32,33) to low frequency sound (< 60 Hz). Our data show that these low frequencies contain important information. Nevertheless, the skilled clinician may often estimate at the bedside the extent of aortic stenosis. Equipped with the additional information shown in our study that poststenotic dilation lowers the frequency of the murmur, the clinician may be able to improve the degree of accuracy of bedside diagnosis. Although bedside diagnosis remains the prime screening

technique, both graphic recording and spectral analysis of the murmur increase the objectivity and sensitivity of diagnosis. Furthermore, objective recordings allow ready comparison of the extent of stenosis over time and facilitate follow-up study of patients.

Finally, our results suggest the possibility that some patients with signs or symptoms of aortic stenosis may be followed up by spectral murmur analysis and echocardiography without the need for invasive testing. For instance, those patients with a low and some asymptomatic patients with an intermediate spectral ratio and normal aortic root dimension may be followed up by the noninvasive techniques. In contrast, in patients with an aortic murmur with a high spectral ratio or in those with an intermediate ratio who are symptomatic or have poststenotic dilation, invasive confirmation of the extent of disease is warranted.

References

1. Perloff JK. Clinical recognition of aortic stenosis. The physical signs and differential diagnosis of the various forms of obstruction to left ventricular outflow. Prog Cardiovasc Dis 1968;10:323–52.
2. Baker C, Somerville J. Clinical features and surgical treatment of fifty patients with severe aortic stenosis. Guy's Hosp Rep 1959;108: 101–11.
3. Lewes D. Diagnosis of aortic stenosis. Br Med J 1951;1:211–6.
4. Björk VO, Malstrom G. The diagnosis of aortic stenosis. Am Heart J 1955;50:303–15.
5. Flohr KH, Weir EK, Chesler E. Diagnosis of aortic stenosis in older age groups using external carotid pulse recording and phonocardiography. Br Heart J 1981;45:577–82.
6. Lyle DP, Bancroft WH, Tucker M, Eddleman EE. Slopes of the carotid pulse wave in normal subjects, aortic valvular diseases and hypertrophic subaortic stenosis. Circulation 1971;63:374–81.
7. Voelkel AG, Kendrick M, Pietro DA, et al. Noninvasive tests to evaluate the severity of aortic stenosis. Chest 1980;77:155–60.
8. Bonner AJ, Sacks HN, Tavel ME. Assessing the severity of aortic stenosis by phonocardiography and external carotid pulse recordings. Circulation 1973;68:247–52.
9. Bonner AJ, Tavel ME. Systolic time intervals. Arch Intern Med 1973;132:816–9.
10. Benchimol A, Dimond EG, Shen Y. Ejection time in aortic stenosis and mitral stenosis. Am J Cardiol 1960;6:728–35.
11. Siegel RJ, Roberts WC. Electrocardiographic observations in severe aortic valve stenosis: correlative necropsy study to clinical, hemodynamic, and ECG variables demonstrating relation of 12-lead QRS amplitude to peak systolic transaortic pressure gradient. Am Heart J 1982;103:210–21.
12. DeMaria AN, Bommer W, Joye J, Lee G, Bouteller J, Mason DT. Value and limitations of cross-sectional echocardiography of the aortic valve in the diagnosis and quantification of valvular aortic stenosis. Circulation 1980;62:304–12.
13. Reichek N, Devereux RB. Reliable estimation of peak left ventricular systolic pressure by M-mode echographic-determined end-diastolic relative wall thickness: identification of severe valvular aortic stenosis in adult patients. Am Heart J 1981;103:202–9.
14. Godley RW, Green D, Dillon JC, Rogers EW, Feigenbaum H, Weyman AE. Reliability of two-dimensional echocardiography in assessing the severity of valvular aortic stenosis. Chest 1981;79:657–62.
15. DePace NL, Ren J-F, Iskandrian AS, Kotler MN, Hakki A-H, Segal BL. Correlation of echocardiographic wall stress and left ventricular pressure and function in aortic stenosis. Circulation 1983;67:854–9.
16. Hatle L, Angelsen BA, Tromsdal A. Non-invasive assessment of aortic stenosis by Doppler ultrasound. Br Heart J 1980;43:284–92.
17. Young JB, Quinones MA, Waggoner AD, Miller RR. Diagnosis and quantification of aortic stenosis with pulsed Doppler echocardiography. Am J Cardiol 1980;45:987–94.
18. Stamm RB, Martin RP. Quantification of pressure gradients across stenotic valves by Doppler ultrasound. J Am Coll Cardiol 1983;2: 707–18.
19. Berger M, Berdoff RL, Gallerstein PE, Goldberg E. Evaluation of aortic stenosis by continuous wave Doppler ultrasound. J Am Coll Cardiol 1984;3:150–6.
20. Johnson GR, Adolph RJ, Campbell DJ. Estimation of the severity of aortic valve stenosis by frequency analysis of the murmur. J Am Coll Cardiol 1983;1:1315–23.
21. Hewlett Packard Application Note AN712 for 8800 Medical System. July 1972.
22. Johnson GR, Myers GS, Lees RS. Quantitative effects of transducer application in phonocardiography (abstr). Circulation 1983;68(suppl III):III-309.
23. Gorlin R, Gorlin SJ. Hydraulic formula for calculation of the area of the stenotic mitral valve, other cardiac valves and central circulatory shunts. Am Heart J 1951;41:1–29.
24. BMDP Program Health Sciences Computing Facility UCLA, sponsored by the NIH Special Research Resources Grant RR-33. Program revised April 1982.
25. Arani DT, Carleton RA. Assessment of aortic valvular stenosis from the aortic pressure pulse. Circulation 1967;36:30–5.
26. Nanda NC, Gramiak R, Shah PM. Echocardiographic misdiagnosis of severity of mitral stenosis (abstr). Clin Res 1975;23:119A.
27. Chang S, Clements S, Chang J. Aortic stenosis: echocardiographic cusp separation and surgical description of aortic valve in 22 patients. Am J Cardiol 1977;39:499–504.
28. Romero M, Nakamura T, Milanes J, Hultgren H. Non-invasive evaluation of severity of aortic stenosis by a point score system and a clinical algorithm (abstr). J Am Coll Cardiol 1984;3:558.
29. Frank S, Johnson A, Ross J. Natural history of valvular aortic stenosis. Br Heart J 1973;35:41–6.
30. Carabello BA, Barry WH, Grossman W. Changes in arterial pressure during left heart pullback in patients with aortic stenosis: a sign of severe aortic stenosis. Am J Cardiol 1979;44:424–7.
31. Clark C. The fluid mechanics of aortic stenosis—I. Theory and steady flow experiments. J Biomech 1976;9:521–8.
32. McKusick V. The auditory mechanism. In: Cardiovascular Sound in Health and Disease. New York: Grune & Stratton, 1958:64–7.
33. Butterworth J, Chassin M, McGrath R. Importance of cardiac auscultation audio-visual equipment. In: Cardiac Auscultation Including Audio-Visual Principles. New York: Grune & Stratton, 1955:15–25.